nature physics

SUPPLEMENTARY INFORMATION

https://doi.org/10.1038/s41567-018-0080-5

In the format provided by the authors and unedited.

Ultrafast preparation and detection of ring currents in single atoms

Sebastian Eckart[1*], Maksim Kunitski[1], Martin Richter[1], Alexander Hartung[1], Jonas Rist[1], Florian Trinter[1], Kilian Fehre[1], Nikolai Schlott[1], Kevin Henrichs[1], Lothar Ph. H. Schmidt[1], Till Jahnke[1], Markus Schöffler[1], Kunlong Liu[2], Ingo Barth[2], Jivesh Kaushal[3], Felipe Morales[3], Misha Ivanov[3], Olga Smirnova[3,4] and Reinhard Dörner[1*]

[1]Institut für Kernphysik, Goethe-Universität Frankfurt am Main, Frankfurt am Main, Germany. [2]Max Planck Institute of Microstructure Physics, Halle (Saale), Germany. [3]Max Born Institute, Berlin, Germany. [4]Technische Universität Berlin, Berlin, Germany. *e-mail: eckart@atom.uni-frankfurt.de; doerner@atom.uni-frankfurt.de

Supplementary Figure 1

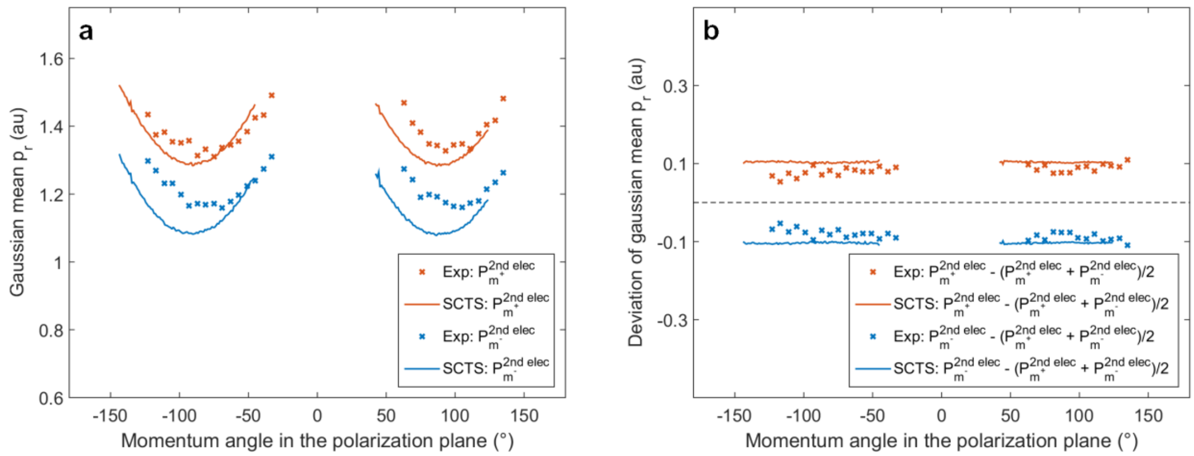

Supplementary Figure 1 | Results of the semiclassical simulation. a, Mean momentum (obtained by fitting a Gaussian distribution and only shown if experimental statistics are sufficient) vs. the momentum angle in the plane of polarization for the experimental data compared to the same quantity from the semiclassical simulations for $m = +1$ (m^+) and $m = -1$ (m^-). **b**, The same as **a** but as deviation to the mean of the m^+ and m^-. Besides a good agreement it is found that the semiclassical simulation slightly overestimates the momentum difference in comparison to the experimental results. This overestimation has its roots in higher differences in the initial transverse momenta for $m = +1$ and $m = -1$ states which are assumed in the semiclassical simulations.

Supplementary Figure 2

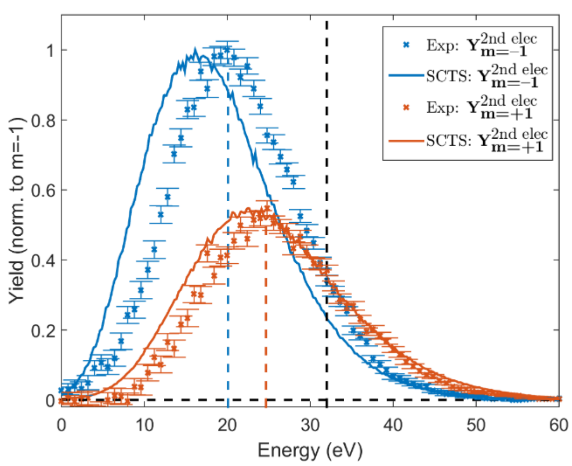

Supplementary Figure 2 | Semiclassical simulation of the electron spectra. Comparison of the experimental results from Fig. 3c with SCTS calculations. The semiclassical simulations assume that the tunneling electron preserves the magnetic quantum number m during tunneling and hence has an initial transverse momentum $p_\perp = m\hbar/r$ at the tunnel exit r. The peaks of the classical distributions are normalized to experimental data. Error bars show the standard deviation of the statistical errors.

Supplementary Figure 3

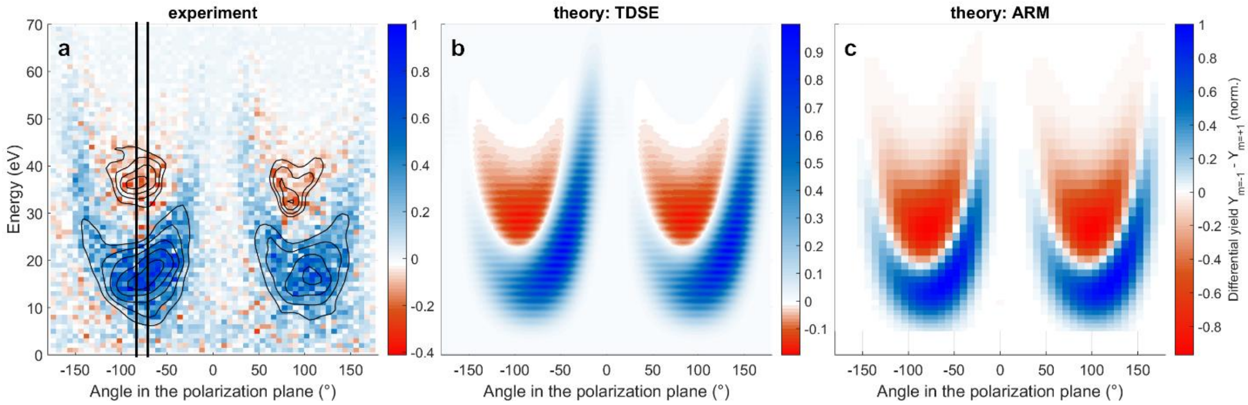

Supplementary Figure 3 | Differences of the m-prepared state's electron momentum distributions. Differential electron momentum distributions $P_{m=-1}^{2nd\ elec} - P_{m=+1}^{2nd\ elec}$ for experiment in **a**, numerical simulation of the time-dependent Schrödinger equation in **b** and analytical R-matrix theory (ARM) in **c**. The differences in the second electron's momenta (created by the probe pulse which is identical in all cases) are caused by the helicity of the pump pulse (which has created the ring current with defined sign in the singly charged ion). The radial differences divide the momentum distribution into a negative region and a positive region. The angular differences (marked with black vertical lines in a) are due to different 'initial' momentum distributions of the electrons tunneling from states $m = -1$ (blue area) and $m = +1$ (red area). Black lines in **a** show contours to guide the eye.

Supplementary Figure 4

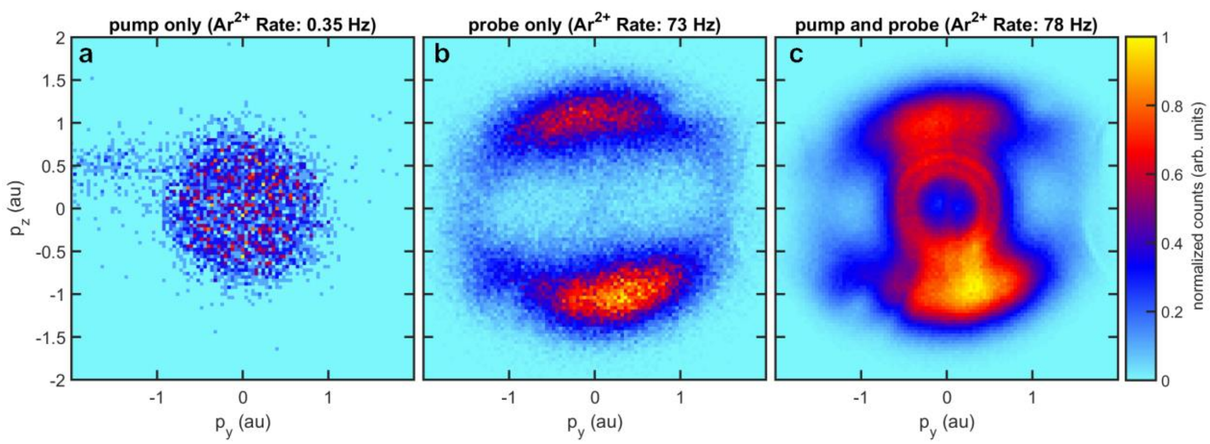

Supplementary Figure 4 | Electron momentum distributions measured in coincidence with Ar^{2+}. a, Normalized electron momentum distribution in the plane of polarization recorded using only the pump pulse. b is the same as a but only the probe pulse was used and in c pump and probe pulse were both used. It can be seen that only pump and probe pulse together are able to produce electrons with $|p_z|<0.5$ au efficiently. We have checked that electrons from the probe pulse alone that would contribute to the final energy spectrum and fulfilling |p_z_calc|<0.5 au are eliminated by the subtraction of random coincidences. Above each distribution the detection rate of Ar^{2+} is shown for the corresponding case which is negligible for the case where there is only the pump pulse.